

## Applicability of urban streets as temporary open floodways


Thea Ingeborg Skrede, Tone Merete Muthanna  and Knut Alfredesen

### ABSTRACT

Climate change coupled with urbanization and its increasing impervious surfaces have caused major challenges for the water sector worldwide. In Norway, an ageing infrastructure with already insufficient drainage capacities results in large amounts of runoff during high-intensity rainfall events causing frequent floods in urban areas. Due to limited available space to handle the future projected increase in stormwater, there is a need to utilize already occupied space for stormwater management, such as roads and streets, during extreme events. Limited research has been done on the design and applicability of urban streets as temporarily flood ways diverting stormwater to the nearest recipient. This paper will study the benefits and limitations of adapting urban streets as safe flood ways to route stormwater by modelling an urban street as a floodway. Streets as floodways will require additional hydraulic performance criteria and safety criteria. Performance criteria are identified and evaluated, and a method is proposed for the evaluation of urban streets applicability as floodways. The method can be used to evaluate the applicability of multifunctional streets used as urban floodways and can be adapted by municipalities as a decision support tool for stormwater management.

**Key words** | floodways, HEC-RAS, hydraulic modelling, stormwater management, urban drainage, urban flood modelling

Thea Ingeborg Skrede (corresponding author)

Tone Merete Muthanna 

Knut Alfredesen

Department of Civil and Environmental Engineering,

The Norwegian University of Science and Technology (NTNU),

Trondheim, Norway

E-mail: [thea.i.skrede@ntnu.no](mailto:thea.i.skrede@ntnu.no);

[thea.ingeborg.skrede@norconsult.com](mailto:thea.ingeborg.skrede@norconsult.com)

### INTRODUCTION

Climate change coupled with urbanization and increasing impervious surfaces have caused major challenges for the water sector worldwide due to the increasing magnitude and frequency of floods (Palmer *et al.* 2008; Ryberg *et al.* 2012; Hirabayashi *et al.* 2013). Climate change in Norway is expected to increase both the intensity and frequency of precipitation (Hanssen-Bauer *et al.* 2017). This, coupled with urbanization, will result in more frequent pluvial flooding and challenges for stormwater management in urban areas (Nilsen *et al.* 2011). An expected increase in surface runoff from extreme events, both in total volume and

peak runoff rates, will result in: flooding due to insufficient drainage capacities; degradation of ecological and biological systems; and pollution from combined sewer overflows (CSO) (Nie 2016). Norway has adopted a three-stage approach to stormwater management introduced by Lindholm *et al.* (2008) and refers to three levels of solutions depending on the rainfall intensity and volume. The first stage applies to everyday events, which should be infiltrated locally, the second stage refers to medium events, and the aim is to detain the water delaying the flood peak and subsequent runoff response. The third stage is for extreme events, where the aim should be to secure safe flood paths. In urban areas, unoccupied and available surface area are often scarce; hence, there is a need to look for existing space which can be utilized for stormwater transport during extreme events.

This is an Open Access article distributed under the terms of the Creative Commons Attribution Licence (CC BY-NC-ND 4.0), which permits copying and redistribution for non-commercial purposes with no derivatives, provided the original work is properly cited (<http://creativecommons.org/licenses/by-nc-nd/4.0/>).

doi: 10.2166/nh.2020.067

Mark *et al.* (2004) note that urban surfaces often are characterized by obstacles such as building, sidewalks, road camber, and drains; hence, lack of accurate representation of these drastically alter surface water flow paths (Hunter *et al.* 2008; Turner *et al.* 2013). In addition, head losses due from flows over or around such features are particularly difficult to represent and simulate (Vojinovic & Tutulic 2009). Hence, models for urban flood analysis require a high spatial resolution (<5 m) to simulate complex flow paths and blockage effects (Vojinovic & Tutulic 2009; Fewtrell *et al.* 2011; Turner *et al.* 2013). Mark *et al.* (2004) recommend a grid resolution of 1–5 m (Mark *et al.* 2004). Since surface flow is strongly influenced by topography and obstacles, digital elevation models at appropriate resolutions are central to simulate urban water surface flow (Noh *et al.* 2018). Hunter *et al.* (2008) found that terrain data available from modern airborne laser scanning, also referred to as ‘Light Detection And Ranging’ (LIDAR) systems, are sufficiently accurate for simulating urban flows. However, result accuracy is not always increased by higher grid resolution, as limitations and uncertainties always will affect flood modelling (Dottori *et al.* 2013).

Urban flooding has been analysed by several authors using one-dimensional (1D; Mark *et al.* 2004; Guillén *et al.* 2017) and two-dimensional (2D) models (Mignot *et al.* 2006; Hunter *et al.* 2008; Fewtrell *et al.* 2011) or coupled 1D/2D models considering dual drainage (Vojinovic & Tutulic 2009; Russo *et al.* 2012; Noh *et al.* 2018). Several authors have investigated the phenomena of flooding on urban streets (Mark *et al.* 2004; Mignot *et al.* 2006; Gomez-Valentin *et al.* 2009), street flooding at very fine resolutions (Ozdemir *et al.* 2013; de Almeida *et al.* 2018), ability of different resolutions to accurately represent street cross-sections and street networks (Mignot *et al.* 2006; Ozdemir *et al.* 2013) or flow at street junctions (Mignot *et al.* 2006, 2008). Guillén *et al.* (2017) used HEC-RAS 1D and large-scale particle image velocimetry to study the velocity distribution in a street cross-section and calibrated the results with amateur videos of an urban flash flood. de Almeida *et al.* (2018) note that the road network can be particularly efficient in transporting water across the urban area and therefore plays an important role.

Numerical flood models are important tools for understanding flood events, flood hazard assessment, and flood

management planning (Patel *et al.* 2017). Typically, model flow parameters (i.e. flow depth, flow velocity and flood duration; Merz *et al.* 2010) are used to evaluate flood hazard. The potential for damages to people, vehicles, buildings, and infrastructure is often assessed using the concept of flood hazard. In literature, there is a conventional agreement that there is a relationship between the hazard level for people exposed to a flood and the depth and velocity in flood water (Abt *et al.* 1989; Lind *et al.* 2004; Russo *et al.* 2013; Luca *et al.* 2015). Most authors have suggested a relationship between the depth–velocity product ( $yv_c$ ) and human stability in water (Abt *et al.* 1989; Lind *et al.* 2004; Russo *et al.* 2013; Luca *et al.* 2015). For pedestrians, a safety threshold of  $(v \times y) = 0.22$  (m<sup>2</sup>/s) is suggested (Martínez-Gomariz *et al.* 2016). However, there is, to the authors’ knowledge, no studied conducted on the use of urban streets as temporary floodways in the context of urban stormwater management.

In this study, a methodology for this is proposed, with the following specific objectives:

- Evaluate the grid placement and density.
- Investigate the most important hydraulic performance criteria for an urban street used as a temporary floodway.
- Investigate the hazard criteria for safe floodways in urban streets.

## METHODS AND MATERIALS

The Damsgård area is located in Puddefjord, Bergen, a city on the west coast of Norway with a cool and wet climate (2,550 mm/year; Jonassen *et al.* 2013). The study area is characterized by steep slopes, ranging from 0 to 468 m above datum NN2000, mostly vegetated with grassland and forests, disconnected from the fjord by a strip of the urban area. A map of the area is presented in Figure 1. Large amounts of runoff from the vegetated steep hillside, in addition to impervious surface in the urban area, cause extensive flash floods and frequent CSOs to the Puddefjord. Bergen municipality is investigating different adaption measures to reduce the flash floods and CSOs to the fjord. One measure is to divert runoff from the upland areas before it reaches the urban area and route it to the fjord as an open floodway in the existing street network.

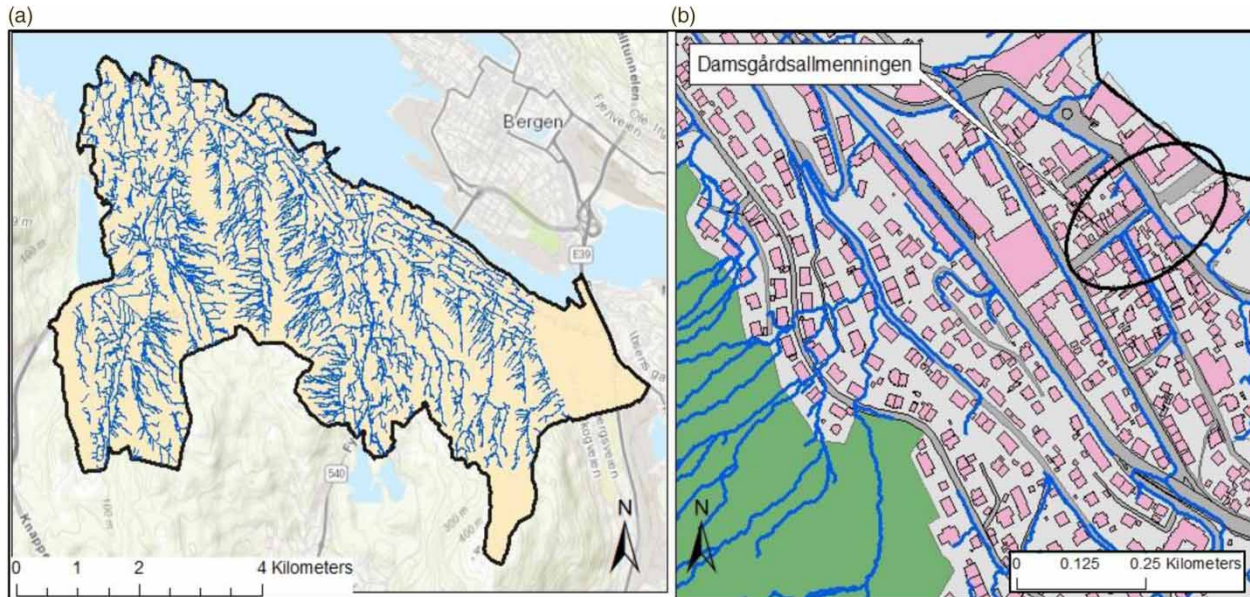


**Figure 1** | The catchment of Damsgård and the placement of the street of Damsgårdsallmenningen. (a) The catchment of Damsgård with drainage lines. (b) The street of Damsgårdsallmenningen and the placement in relation to exiting drainage lines.

The street of Damsgårdsallmenningen is suggested as an applicable street segment for this study based on the following suitability: (1) it is a straight segment leading directly to a recipient; (2) the stormwater runoff from a large sub-watershed could easily be routed into the street; (3) the street segment includes intersections and is widely used for parking, which allows for flow evaluations of common urban situations; (4) the street has a typical cross-section with sidewalks on both sides and (5) is located in an area with frequent flooding problems. Watersheds A and B (Figure 2) are considered suitable areas from which stormwater runoff could be routed to Damsgårdsallmenningen.

For the purpose of this study, it is assumed that the drainage system is operating at full capacity, and that stormwater on the surface does not interact with the sewer network. Travel time or transport from the watershed to the street is not considered, in addition to the design of the transportation solution from the watershed outlet to the Damsgårdsallmenningen. It was assumed that there were no moving vehicles or pedestrians in the street during the flood event.

For this study, a digital surface model (DSM) of the street and surroundings in the resolution  $0.1\text{ m} \times 0.1\text{ m}$  is rasterized from LIDAR data in ArcMap 10.6; for the entire study site, a digital terrain model (DTM) and a DSM in

the resolution of  $1.0\text{ m} \times 1.0\text{ m}$  were accessed from the Norwegian Mapping Authority online database (Hoydedata 2018). Precipitation intensity and return periods are obtained for the Florida gauge station in Bergen from the Norwegian Meteorological Institute (Eklima 2018).

The precipitation events for modelling were calculated using hyetographs as input, to ensure that the high-intensity minutes of a storm with variable intensity were represented in a hyetograph for 1 h rainfall event derived from IDF curves (Kristvik et al. 2018). Two watersheds, Watersheds A and B, were defined based on topography and drainage lines. The two watersheds were split into sub-basins based on isochrones and drainage lines. Isochrones of equal travel time were constructed based on the topography and response time of the watershed, where concentration is used as an appropriate representation of response time (Singh 2005).

Time of concentration is found using the method introduced by Kirpich in 1940 for channel flow and Kerby in 1959 for overland flow. Runoff is assumed to flow as overland flow until the lower boundary of the watersheds, where it is routed to the outlet of the watershed in an open channel, where water is transported to the street. Watersheds A and B were divided into four and six sub-basins, respectively. Watershed A represents the area

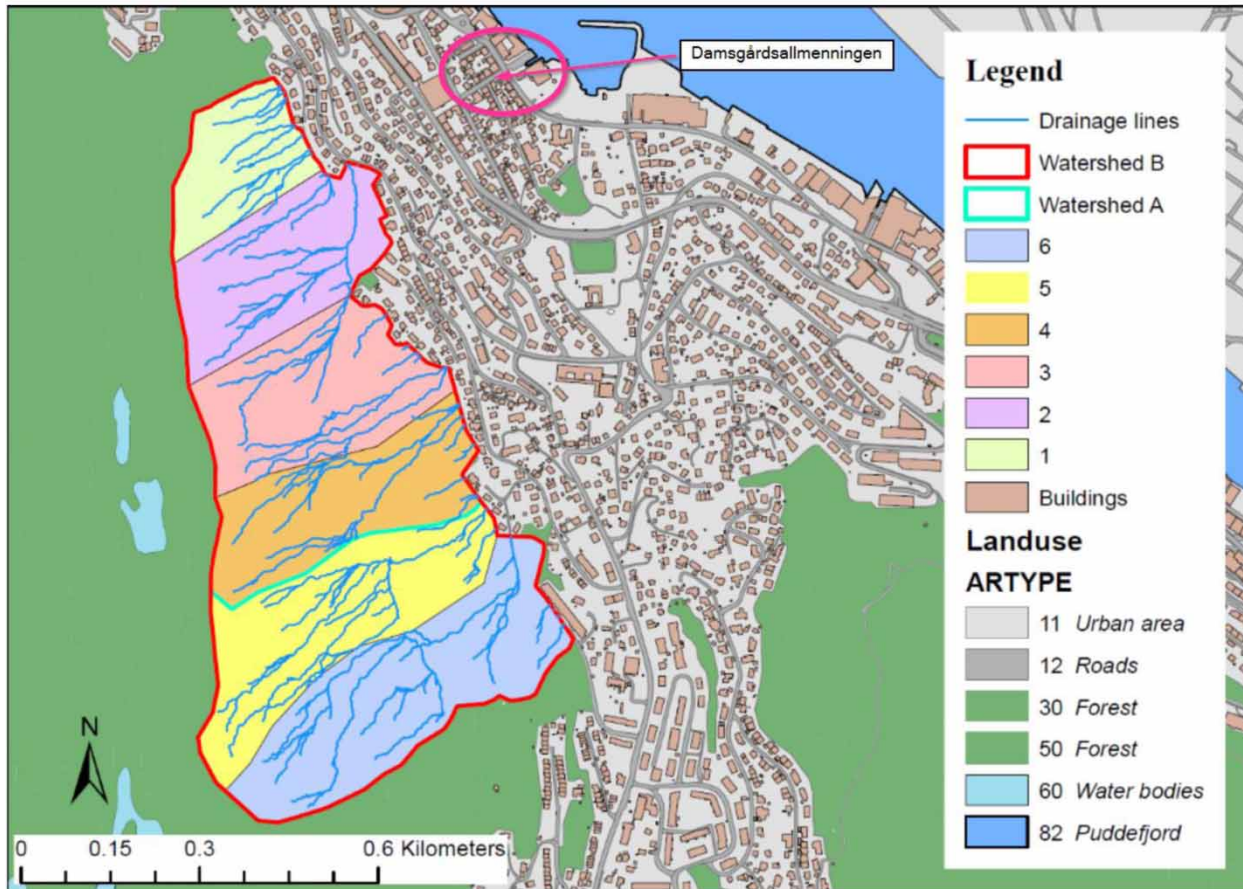


**Figure 2** | The placement of Watersheds A and B in relation to the street of Damsgårdsallmenningen. Watershed B consists of sub-basins 1–6 and Watershed A consists of sub-basins 1–4.

contribution to runoff to Damsgårdsallmenningen, and Watershed B is an extension of Watershed B. Table 1 presents the study site characteristics and the watersheds' responses. The length of overland flow and the length of channel were found for each sub-basin of the watersheds

using a DTM with a resolution of 1.0 m\*1.0 m and the measure tool in ArcMap. The slope of the channel and the sub-basins were found using 3D analyst in ArcGIS. Times of concentrations are 33.5 and 27.8 min for Watersheds B and A, respectively.

**Table 1** | Study site characteristics

Area	Size	Land use	Slope (°)	Runoff travel distance	Response time (min)
Damsgård	34.389 194 km <sup>2</sup>	Built-up 48.3%, Forest 44.2% Open land 4.8%	–	–	–
Watershed A	276,319 m <sup>2</sup>	Forest 100%	Minimum = 0.14, Maximum = 86.22 Average = 52.29	$L = 785$ m	$T_c = 27.8$
Watershed B	481,036 m <sup>2</sup>	Forest 100%	Minimum = 0.010, Maximum = 86.22 Average = 48.05	$L = 1,132$ m	$T_c = 33.5$

Combining the rational method with mathematical convolution into what is commonly called the time–area–method (Butler & Davies 2004) allows for the generation of flow hydrographs. A synthetic hydrograph was created for each watershed according to the time–area method. Abstractions from storage and infiltration were included in the runoff coefficient (Villarreal *et al.* 2004). A conservative runoff coefficient of 0.5 for the vegetated area was used due to steep slopes and high-intensity precipitation resulting in low infiltration. The soil is assumed not saturated from previous precipitation events (Bergen kommune 2005). The pipe that drains the watershed is a 0.40 m smooth concrete pipe with a slope of 100 mm/m, and is assumed to have a capacity of 650 l/s.

The capacity of the overflow is extracted from the hydrograph, as demonstrated in Figure 4. Runoff exceeding 650 l/s is assumed to be overland flow Damsgårdsallmenningen.

For the modelling HEC-RAS 5.0.4, 2D with a full momentum equation with up to 40 iterations was used. Due to low roughness on urban asphalt, steep slopes, confined wetted perimeter and known cases of flash flooding in the area, the full momentum was used for the analysis to more accurately simulate rapid changes in velocity. The stability of the numerical computations is strongly dependent on the relationship between the time step, grid size, and maximum iterations. The Courant–Friedrichs–Lewy condition was used to optimize the grid size and time step

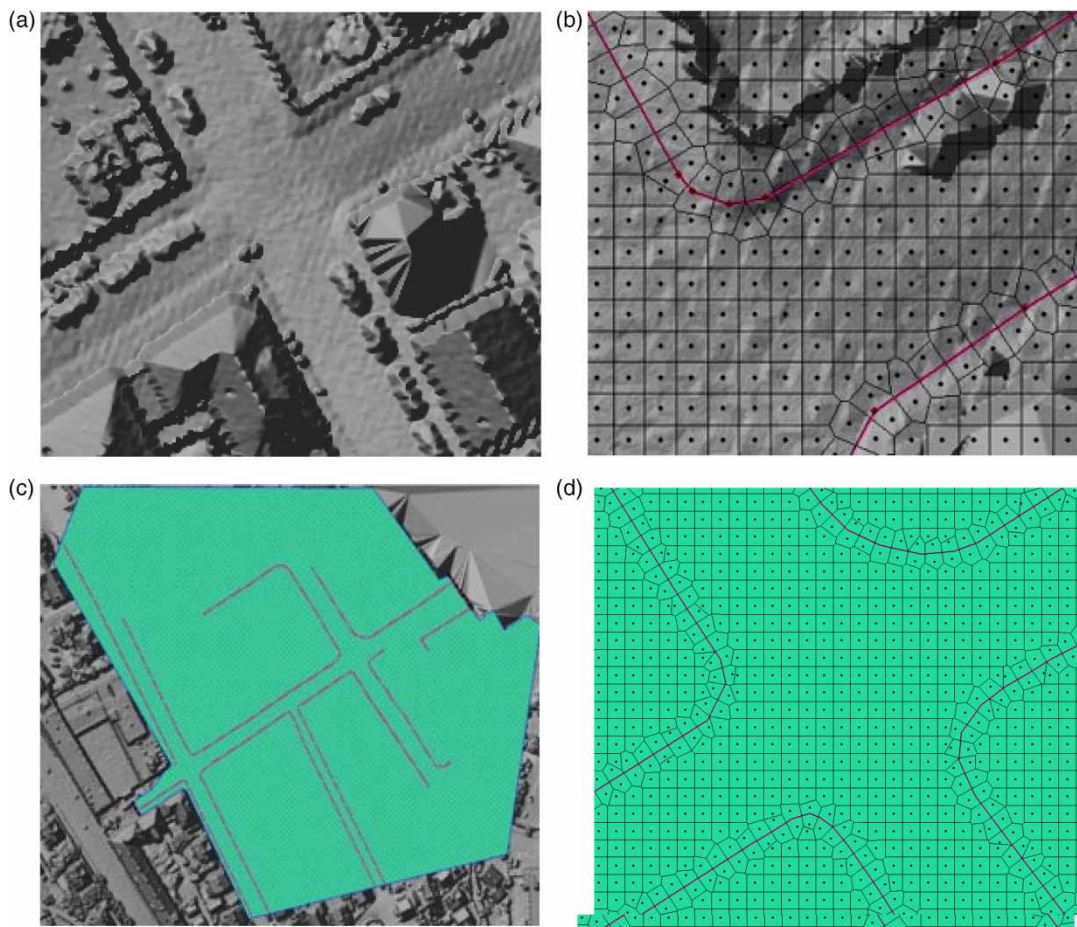


**Figure 3** | Overview of computational grid mesh and grid cells for the modelled street (shown as black-circled area in Figure 1). (a) Terrain resolution with the presence of urban obstacles represented by parked vehicles. (b) Grid coverage over urban obstacles with break lines with a resolution of 1 m\*1 m. (c) Break lines placement within the computational grid of resolution of 1 m\*1 m. (d) Break lines with cell face alignment in the computational grid of resolution of 1 m\*1 m.

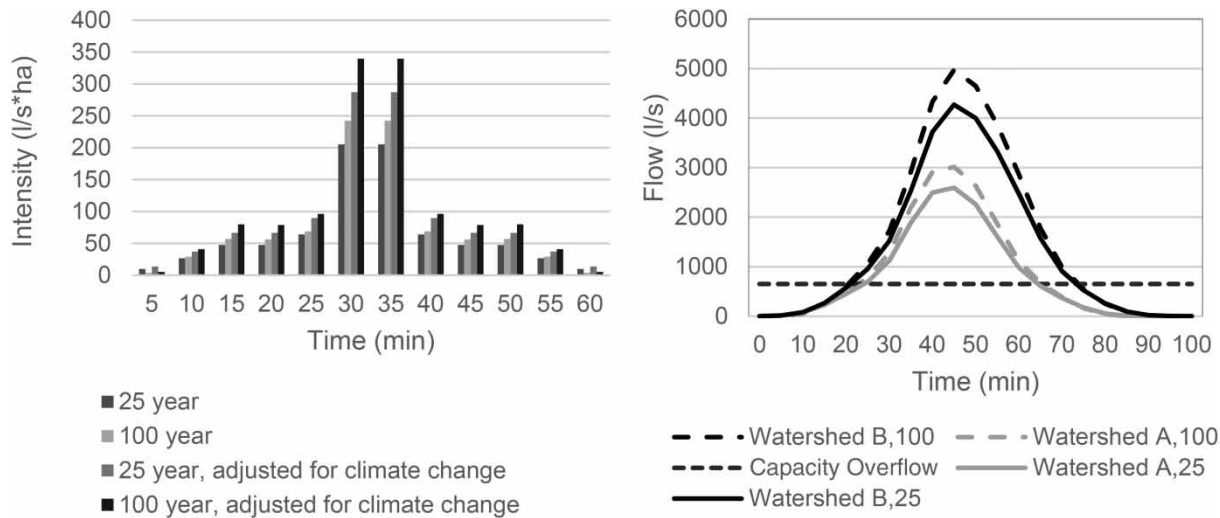


**Figure 4** | Design storm hyetograph with 25- and 100-year return periods on the left-hand side, and resulting hydrograph routed into the floodway to the right.

for shallow water flows (Brunner 2016):

$$Cr = \frac{v \Delta t}{\Delta x} \leq 1 \quad (1)$$

or

$$\Delta x \leq \frac{v \Delta t}{Cr} \quad (\text{with } Cr = 1.0) \quad (2)$$

where  $Cr$  is the Courant number,  $v$  is the flood wave velocity (m/s),  $\Delta t$  is the computational time step (s) and  $\Delta x$  is the grid resolution (m). The 2D model was set up using a computational domain defined by a closed polygon, with a computational mesh generated from grid cells within the domain boundary. The computational cells may be arranged in a staggered or a non-staggered grid composed of polygons between three sides and eight sides (Moya Quiroga et al. 2016). The computational mesh is drawn on an underlying terrain model with a resolution of 0.10 m\*0.10 m. The terrain is extracted from LIDAR data and rasterized into a 0.1 m\*0.1 m DSM in ArcMap by using the ‘LAS to raster’ tool without removing first return and surface features. The extremely fine resolution is chosen to capture velocity around urban features such as vehicles and curb design. The computational domain (2D mesh) was constructed of a total 29,810 cells, from a staggered grid composed of rectangular cells 1 m\*1 m, which generated a grid with the

maximum cell size of 1.85 m<sup>2</sup>, a minimum cell size of 0.3 m<sup>2</sup> and an average cell size of 0.98 m<sup>2</sup>, see Figure 3.

Different placements and shapes of the mesh were evaluated to test the sensitivity of grid placement to ensure that waterflow was not disrupted by the border of the computational grid. Break lines were placed along the edge of the sidewalk (curb) to ensure cell face alignment with the terrain difference between street and sidewalk.

It was assumed that gutters, roof, and streets did not significantly contribute to the runoff volume compared with the large upstream catchment area. If the precipitation volume falling on the studied area is small compared with the input hydrographs volumes, their effects will be very small (Mignot et al. 2006). Only the synthetic hydrograph is used as the boundary condition, since the volume from precipitation on the street is also assumed negligible, due to the small area contributing compared with runoff from the watershed.

The roughness coefficient of the entire area is set to 0.016, as suggested for rough asphalt (Chow 1959). The roughness coefficient is the most common calibration parameter used in HEC-RAS 2D modelling. As no observed flow can be used for calibration, a sensitivity analysis was performed with different roughness coefficient values to test the model sensitivity for roughness coefficients and the corresponding uncertainty in the results. Higher Manning’s values resulted in lower velocities but did not affect the results and the value of 0.016 chosen.

The open floodway would be activated for precipitation events not handled by the sewage system in Bergen, which is designed for 20 years. Therefore, a design storm of the 25-year return period was chosen to model the effect of a small storm exceeding the overflow ( $O_{\text{watershed}}$ ) capacity.

In addition, a 100-year storm was used to evaluate the floodway performance during an extreme event. A climate factor of 1.4, to account for an expected climate change in the design, is applied to precipitation data from Florida, which is the recommended climate factor for durations less than 3 h for Hordaland county (Kristvik *et al.* 2018). Design storm hyetographs were constructed for a 25- and a 100-year return period and are presented in Figure 4.

The model was run for two different flooding scenarios: 25-year and 100-year return periods. The time step was 0.1 s for all the simulations, which was the smallest time step available in HEC-RAS 5.0.4 during the simulations. Finally,

the product of the resulting water velocities ( $v$ ) and water depths ( $h$ ) in addition to maximum velocities were analysed for each watershed and the return period to evaluate the impact of using the street as an open floodway.

## RESULTS AND DISCUSSION

With the implementation of infiltration and retention measures from steps 1 and 2 in the three-step strategy for stormwater management (Lindholm *et al.* 2008), abstractions should be subtracted from the stormwater hydrograph. The synthetic input hydrographs represent the direct runoff that is considered routed to the street segment included abstractions from overflow and stormwater management measures.

Figure 5 presents maximum velocity conditions for a storm with 60-min duration with 25- and 100-year return

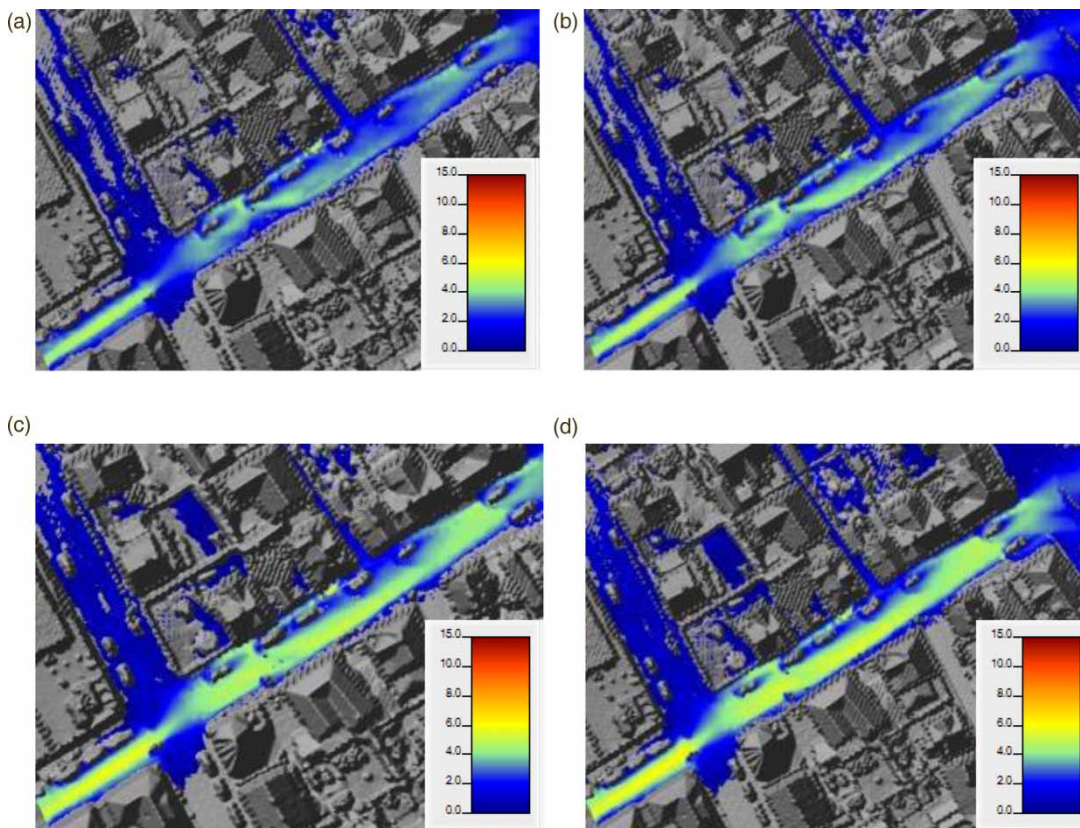


**Figure 5** | Maximum velocity simulated in the street segment for different return periods and contributing areas. (a) Maximum velocity distribution (m/s) in the street with runoff from Watershed A for a 60 min storm with  $T = 25$  years. (b) Maximum velocity distribution (m/s) in the street with runoff from Watershed A for a 60 min storm with  $T = 100$  years. (c) Maximum velocity distribution (m/s) in the street with runoff from Watershed B for a 60 min storm with  $T = 25$  years. (d) Maximum velocity distribution (m/s) in the street with runoff from Watershed B for a 60 min storm with  $T = 100$  years.

periods for each Watershed A and B. In Figure 5, velocities are used to represent the hazard potential in the street for the evaluation of pedestrian safety and to represent flow around vehicles. During the initial stages of the flood, the

maximum hazard conditions were found at the upper boundary of the street, the inlet where stormwater would reach the floodway (Figures 5 and 6). This indicates that the design and placement of the inlet is important, and

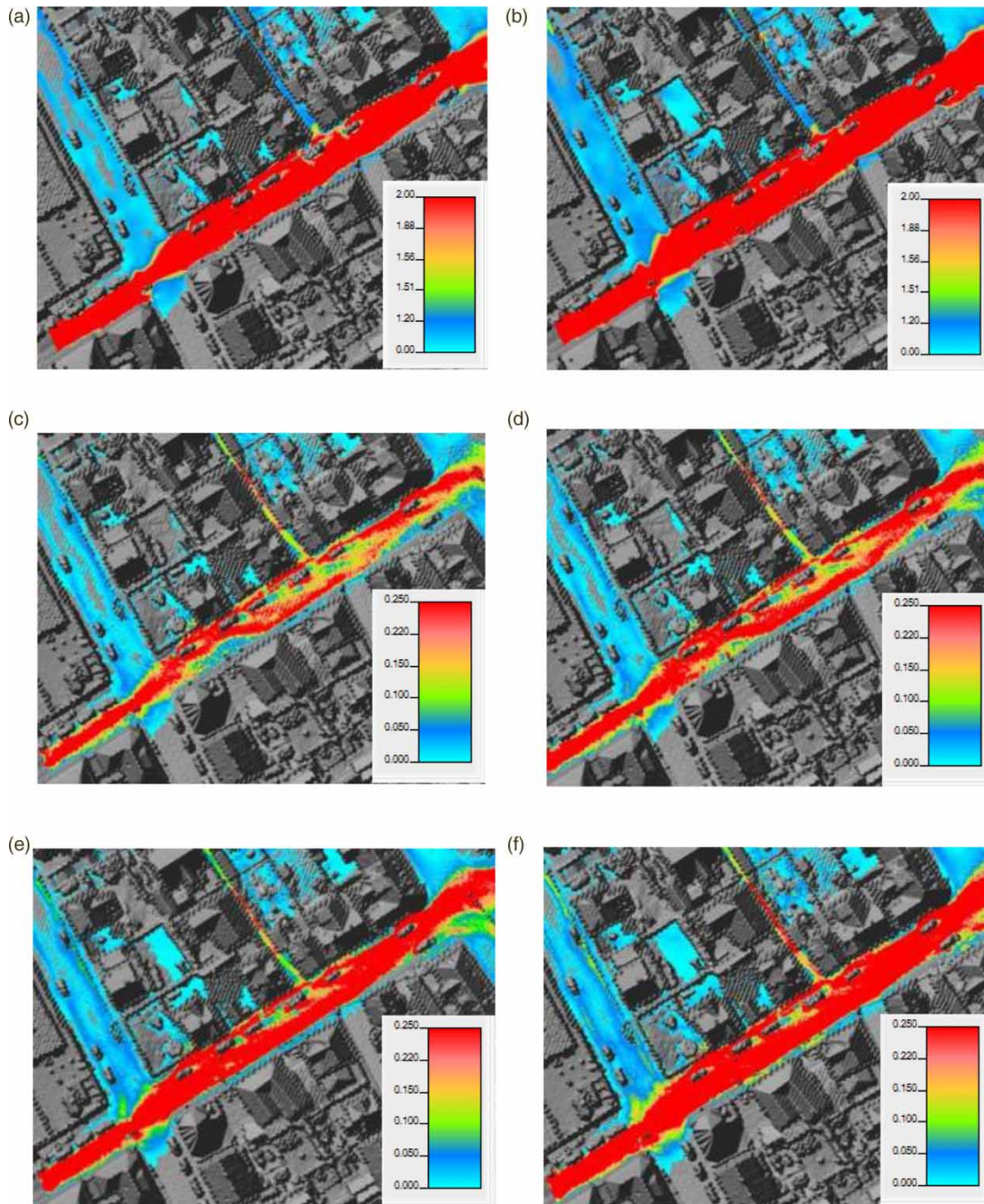


**Figure 6** | Hazard potential in the street for Watershed B with a 100-year return period. (a) Maximum hazard potential from velocity (m/s) in the street from Watershed A,  $T = 100$  years. (b) Maximum hazard potential from velocity (m/s) in the street from Watershed B,  $T = 100$  years. (c) Maximum depth-velocity ( $\text{m}^2/\text{s}$ ) product in the street from Watershed A,  $T = 25$  years. (d) Maximum depth-velocity product ( $\text{m}^2/\text{s}$ ) in the street from Watershed A,  $T = 100$  years. (e) Maximum depth-velocity product ( $\text{m}^2/\text{s}$ ) in the street from Watershed B,  $T = 25$  years. (f) Maximum depth-velocity product ( $\text{m}^2/\text{s}$ ) in the street from Watershed B,  $T = 100$  years.



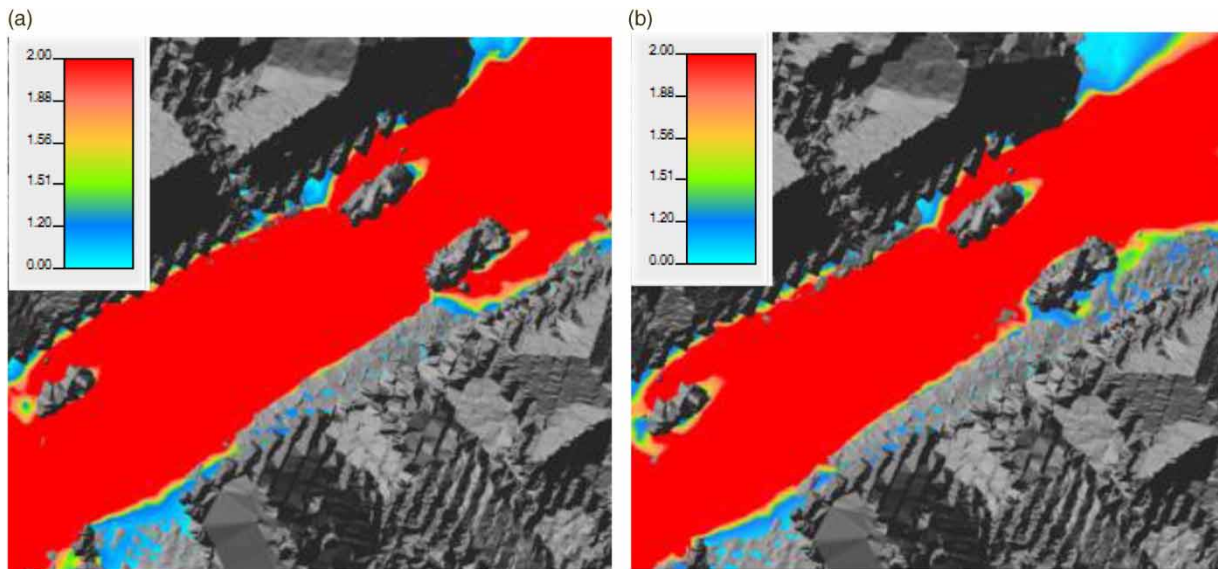


**Figure 7** | Flood velocity as hazard potential around urban obstacles. (a) Hazard (m/s) from Watershed A,  $T = 100$  years. (b) Hazard (m/s) from Watershed B,  $T = 100$  years.

safety measures such as walls and levees should be considered.

The first event ( $T = 100$  years) was used to evaluate if the street could be considered a *Safe* floodway during the design storm. High velocities (in the range of 6–7 m/s) are present; however, these are mainly in the driving lane and behind a larger object such as cars, and lower at the sidewalk (Figure 4). The second event ( $T = 25$  years) was applied to demonstrate flow conditions during a precipitation event, which is just large enough to activate the street.

The event results in velocities in the range of 4–5 m/s, with low depth profiles, which indicates that even for a small storm (i.e.  $T = 25$ ) hazardous velocities are expected; in addition, these happen at relatively low depths.

However, the results indicate that the size of the upstream watershed is an important consideration, as Watershed B results in significantly higher velocities, both in the driving lane and on the sidewalk. This indicates that the use of multiple streets as floodways might be beneficial instead of using one major floodway to reduce maximum flow and velocity. A multiple floodway system would result in a larger total flooded area, but at a lower hazard exposed to the public.

High velocities at low depths are considered more dangerous than high depths coupled with low velocities due to sliding instability (Martínez-Gomariz et al. 2016).

The depth–velocity product threshold in the street is less affected by depth due to the magnitude of the peak velocity. Velocity is the dominating parameter in hazard potential, which is also evident in Figure 6. However, there are some cases where the depth–velocity would indicate hazard where only maximum velocity does not. This indicates the importance of considering more than one hazard threshold. The total hazard area should consider a union of both.

Using the hazard criteria with low hazard ( $v = 1.51$  m/s) corresponds to a maximum depth of 0.146 m ( $y_m$ ) if depth–velocity should not exceed  $0.22$  m<sup>2</sup>/s, which is 4.6 cm higher than the maximum depth of 10 cm recommended in the Copenhagen cloudburst management plan (The City of Copenhagen 2012). A maximum depth of 0.1 m results in an allowable velocity of 2.2 m/s, which is significantly larger than 1.51 m/s defined for low hazard. In Norway, curb height varies from 4 to 10 cm, and in this case,  $y_m$  would result in a water surface of 4.6–10.6 cm above the sidewalk and thus exposing basement windows and floor to ceiling windows to the floodway. To avoid this issue, municipalities should aim to design floodways where maximum depth do not affect private properties ( $y_m = \text{curb height} + \text{height from cross fall}$ ).

From Figures 6 and 7, it is evident that flow conditions around parked vehicles induce an elevated hazard potential. This indicates that it would be beneficial with a parking ban

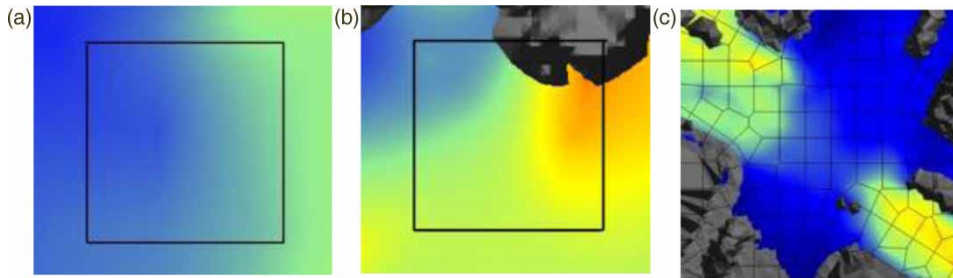


**Figure 8** | Velocity distribution in cells with 2.0 m\*2.0 m grid for with DW using a time step of 0.1 s. (a) Velocity distribution in one 2.0 m\*2.0 m cell with a diffusive wave equation using 0.1 s time step. (b) Velocity distribution around a car with 2.0 m\*2.0 m grid and a diffusive wave equation using 0.1 s time step. (c) Velocity distribution in the grid mesh with 2.0 m\*2.0 m cells and a diffusive wave equation using 0.1 s time step.

on days when high-intensity precipitation is expected. The results show that using a depth-velocity product as hazard criteria, the street segment can only serve as a floodway for Watershed A (27 ha) with parking on both sides of the street. The resolution of the terrain model showed to be important for the model accuracy. In HEC-RAS 2D, the model accuracy is mostly dependent on the resolution of the terrain model, not the computational mesh cell size. Figure 8 demonstrates that HEC-RAS 2D distributes velocity within a mesh cell.

Finer grid cell sizes were considered and tested, but with the HEC-RAS limitation of minimum time step of 0.1 s, the model was not stable for cell size smaller than 1 m\*1 m, as demonstrated by high courant numbers (Table 2). Coarser grid sizes were also tested to evaluate the effect on computational cost and accuracy.

The evolution of water depths and velocity at two representative control points throughout the simulation using the

diffusive wave approximation and the full momentum equation at grid resolutions of 0.2, 0.5, 1, 1.5 and 2 m were used to investigate the numerical stability of the model. The diffusive wave is more stable at a higher courant number than the full momentum (Brunner 2016). The difference in velocities is greater than the difference in depths for both equations for all sets excluding the full momentum with cell size 0.2 m\*0.2 m, which appeared to be convergent. It was evident that the relative difference in depths from the diffusive wave is of a lesser magnitude than with the full momentum at different grid sizes. As noted in previous studies on urban flooding, there is noticeable reduction in model performance at very fine-grid resolutions up to 1 m over the entire domain in this case.

Resolutions 2.0 and 1.5 m do not properly represent the wetting front for both equations, thus resulting in a rapid increase in velocity at 30–35 min compared with the slow build-up at 20 min with the other resolutions.

**Table 2** | Model parameters from grid-sensitivity analysis for Watershed B with a 100-year return period

Cell size (m*m)	Number of cells	Equation set	Time step (s)	Run time (hh:mm:ss)	Maximum velocity (m/s)	Courant number
0.2*0.2	732,953	Full momentum	0.1	58:25:23	13.5	6.75
0.5*0.5	117,038	Full momentum	0.1	05:23:14	6.7	1.34
1.0*1.0	29,810	Full momentum	0.1	01:25:28	6.5	0.65
1.5*1.5	13,574	Full momentum	0.1	00:49:53	6.5	0.43
2.0*2.0	7,657	Full momentum	0.1	00:29:09	6.4	0.32
0.2*0.2	732,953	Diffusive wave	0.1	25:06:34	10.5	5.25
0.5*0.5	117,038	Diffusive wave	0.1	03:02:58	10.1	2.02
1.0*1.0	29,810	Diffusive wave	0.1	00:40:36	7.48	0.75
1.5*1.5	13,574	Diffusive wave	0.1	00:20:20	7.81	0.52
2.0*2.0	7,657	Diffusive wave	0.1	00:06:55	7.87	0.39

Table 2 and Figure 8 illustrate the importance of a grid size sensitivity test and how the grid size affects the accuracy of the results. In addition, coarser resolutions might yield correct peak velocity, but are not fully able to represent the increase in velocity over time. This study was conducted on a steep street where the local or convective acceleration is expected to affect the results. The results from the different model runs verified that there is a correlation between grid size and inability to simulate velocities. This is likely due to HEC-RAS limitation of minimum 0.1 s time step. This indicates that grid sizes below 1 m are unsuitable for urban modelling in HEC-RAS, and the terrain resolution is more important. The results indicate that for urban areas with rapid water movement, coarser resolution of the computational grid than the terrain is preferred, in contradiction to previous studies where grid size is selected at the same resolution as the underlying terrain (Moya Quiruga *et al.* 2016; Patel *et al.* 2017). For the model to accurately simulate velocity changes in the boundary between the driving lane and the sidewalk. The cell's face should be parallel to the edge of the sidewalk (curb) to induce overflow only when the water depth exceeded the curb height.

Fewtrell *et al.* (2008) note that urban environments often are characterized by high spatial-height variability and the method of grid interpolation, and the elevation model is of great importance, and at a coarser scale greatly affects the building representation (Fewtrell *et al.* 2008). However, HEC-RAS RAS-mapper utilizes a TIN model to describe the terrain, and the triangular representation of the street cross-section does not represent the street as a continuous line. Therefore, the model might overestimate the storing and depression during the wetting front. This could be the reason for the slow build-up of velocities.

A correlation was observed between the presence of urban obstacles and hazard potential; however, it is important to note that in this study, such obstacles were represented as continuous 'walls' where, in reality, the water would flow around the tires and under the body of the vehicle. This could result in substantial lift and pressure conditions under and around the vehicles, whereas in the model, water can only flow around or over the vehicle. A comparison between the DSM and a clean DTM was not conducted in this study but may be done to study the effect of a forecast-based parking ban and to examine how

much the urban objects affect the results, but this is outside the scope of this study.

The delay caused by the transportation of runoff to the street was not considered in this study but should be considered. In addition, the effect of debris or erosion of the street has not been considered. The floodway should be tested with storm events of lower duration than the lag time to simulate a flood from a storm where the rain would have stopped before the floodway is activated – thus, a situation where a pedestrian might not expect flash flooding since it is no longer raining.

At high volume and velocity of runoff, the spillover from the street in the intersections into adjoining streets is evident. This does indicate that the design and layout of intersections is an area of floodways which requires more research, and different designs for the confinement of water and safe crossing could be considered (i.e. use of elevated pedestrian crossing as water levees). The results offer much potential for using urban streets as floodways by routing in street perpendicular to the slope will reduce peak velocity. The findings indicate that even at steep slopes, streets could be suitable as floodways due to the sidewalks curb height effect in reducing hazard conditions. Moreover, floodways might be even more suitable for streets with a lower slope, however, then flood duration and flood intrusion will be important for performance criteria.

---

## CONCLUDING REMARKS

The results presented in this study show that HEC-RAS with a grid size of 1 m\*1 m over a street segment of 146 m is a suitable tool to simulate the use of an urban street as a floodway, however with some limitations. Grid sizes of 0.2 and 0.5 m are unsuitable for urban modelling of street segments in HEC-RAS due to the limitation in time step values lower than 0.1 s, whereas grid sizes above 1.5 m did not represent the wetting front adequately. The results show that the computational grid does not require the same resolution as the terrain, which can save computational cost, but also highlights the need for good terrain models. For modelling of urban flood, the accuracy of the results depends on the underlying terrain and the density of the computational grid sizes. The sensitivity of the results to grid size should

thus be investigated in all projects. To assess how the water moves around minor terrain features and objects, different sizes of computational mesh and grid placement should be tested in each study. For sub-grid modelling of urban flood, cell faces should be parallel to the terrain features.

The study identified several performance criteria for which the applicability of urban streets as floodway should be evaluated. The most important hydraulic performance criteria found were: flood velocity, flood depth, transportation capacity, total flooding extent, flood duration, and activation frequency.

To decide if a floodway can be considered safe, the concept of hazard potential for pedestrians and the public was utilized. The study has identified the importance of using appropriate hazard criteria for the evaluation of hazard potential. Velocity was identified as the dominating factor affecting hazard potential for pedestrians when urban streets are used as a floodway. Other factors affecting the hazard and damage potential of the floodway were flood depth, depth-velocity product, total flooding extent and debris.

It was found that either transportation capacity or hazard potential was the restricting design criteria for an urban street as a temporary floodway. Thus, when planning safe floodways, planners must choose between the level of safety and the hydraulic performance of the floodway. Higher velocities and larger flow increase the hydraulic performance of how much floodwater the street can handle, in addition to increasing the hazard potential. Other findings from the study:

- A correlation between hazard on the street and the presence of urban obstacles (represented as vehicles). Urban obstacles affected flow distribution and increased velocity.
- High hazard potential is found in the street, but due to the curb height a substantial lower velocity is present at the sidewalk, thus indicating that urban streets can be made suitable floodways by the implementation of elevated curbstones.
- Different placement floodways on the street significantly affect the hazard potential. Floodways in urban streets would be safer if they are on streets which are perpendicular to the slope of the terrain, thus resulting in lower velocity and lower hazard potential.

- HEC-RAS is an efficient tool for mapping floodways and identifying existing floodways in the terrain.

The use of steep urban streets as floodways would therefore not be recommended without the substantial implementation of flood safety measures, such as levees or elevated pedestrian crossing, and elevated curbs. Municipalities should include maximum flow depths and velocities in political regulations and design criteria in urban areas, both in open floodways and for surface flow for when only the major system is operational (e.g. sewer at capacity or blockage). The study has demonstrated that there are several suitable hazard criteria for urban environments in the literature (Martínez-Gomariz *et al.* 2016) and that HEC-RAS is a suitable and efficient tool for depth and velocity mapping in urban areas.

## ACKNOWLEDGEMENTS

The present study was made possible by the BINGO project – *Bringing INnovation to onGOing water management – a better future under climate change* (projectbingo.eu) and by Klima 2050, Centre for Research-based Innovation (klima2050.no).

## REFERENCES

- Abt, S., Wittier, R., Taylor, A. & Love, D. 1989 [Human stability in a high flood hazard zone](#). *JAWRA Journal of the American Water Resources Association* 25 (4), 881–890.
- Bergen kommune (The Municipality of Bergen) 2005 *Retningslinjer for overvannshåndtering i Bergen (Guidelines for Stormwater Handling in the Municipality of Bergen)*. Byrådsavdeling for byutvikling og Vann- og avløpsetaten (City Council for City Development and the Water and Wastewater Agency), Bergen, Norway.
- Brunner, G. W. 2016 *2D Modeling User's Manual*. Institute for Water Resources, Hydrologic Engineering Center, Davis, CA.
- Butler, D. & Davies, J. 2003 *Urban Drainage*. Spon Press, London.
- Chow, V. T. 1959 *Open-Channel Hydraulics*. McGraw Hill, New York.
- de Almeida, G. A. M., Bates, P. & Ozdemir, H. 2018 [Modelling urban floods at submetre resolution: challenges or opportunities for flood risk management?](#) *Journal of Flood Risk Management* 11 (S2), S855–S865.
- Dottori, F., Baldassarre, G. D. & Todini, E. 2013 [Detailed data is welcome, but with a pinch of salt: accuracy, precision, and](#)

- uncertainty in flood inundation modeling. *Water Resources Research* **49** (9), 6079–6085.
- Eklima 2018 Available from: <http://eklima.met.no/> (accessed 18 March 2018).
- Fewtrell, T. J., Bates, P. D., Horritt, M. & Hunter, N. M. 2008 Evaluating the effect of scale in flood inundation modelling in urban environments. *Hydrological Processes* **22** (26), 5107–5118.
- Fewtrell, T. J., Duncan, A., Sampson, C. C., Neal, J. C. & Bates, P. D. 2011 Benchmarking urban flood models of varying complexity and scale using high resolution terrestrial LiDAR data. *Physics and Chemistry of the Earth, Parts A/B/C* **36** (7), 281–291.
- Gomez-Valentin, M., Macchione, F. & Russo, B. 2009 Hydraulic behavior of urban streets during storm events. *Ingenieria Hidraulica en Mexico* **24** (3), 51–62.
- Guillén, N. F., Patalano, A., García, C. M. & Bertoni, J. C. 2017 Use of LSPIV in assessing urban flash flood vulnerability. *Natural Hazards* **87** (1), 383–394.
- Hanssen-Bauer, E. J., Haddeland, I., Hisdal, H. & Mayer, S., I.F. 2017 Climate in Norway 2100 – a knowledge base for climate adaptation. NCCS Report. N. E. Agency, The Norwegian Centre for Climate Services. M-741: 204.
- Hirabayashi, Y., Mahendran, R., Koirala, S., Konoshima, L., Yamazaki, D., Watanabe, S., Kim, H. & Kanae, S. 2013 Global flood risk under climate change. *Nature Climate Change* **3** (9), 816.
- Hoydedata 2018 Available from: <https://hoydedata.no/LaserInnsyn/> (accessed 1 March 2018).
- Hunter, N. M., Bates, P. D., Neelz, S., Pender, G., Villanueva, I., Wright, N. G., Liang, D., Falconer, R. A., Lin, B., Waller, S., Crossley, A. J. & Mason, D. C. 2008 Benchmarking 2D hydraulic models for urban flooding. *Proceedings of the Institution of Civil Engineers – Water Management* **161** (1), 13–30.
- Jonassen, M. O., Ólafsson, H., Valved, A. S., Reuder, J. & Olseth, J. A. 2013 Simulations of the Bergen orographic wind shelter. *Tellus A: Dynamic Meteorology and Oceanography* **65** (1), 19206.
- Kristvik, E., Kleiven, G. H., Lohne, J. & Muthanna, T. M. 2018 Assessing the robustness of raingardens under climate change using SDSM and temporal downscaling. *Water Science and Technology* **77** (6), 1640–1650.
- Lind, N., Hartford, D. & Assaf, H. 2004 Hydrodynamic models of human stability in a flood1. *JAWRA Journal of the American Water Resources Association* **40** (1), 89–96.
- Lindholm, O., Endresen, S., Thorolfsson, S., Sægrov, S., Jakobsen, G. & Aaby, L. 2008 Veiledning i klimatilpasset overvannshåndtering. *Norsk Vann. Hamar* **162**, 8–9.
- Luca, M., Marco, P. & Roberto, R. 2015 A conceptual model of people's vulnerability to floods. *Water Resources Research* **51** (1), 182–197.
- Mark, O., Weesakul, S., Apirumanekul, C., Aroonnet, S. B. & Djordjević, S. 2004 Potential and limitations of 1D modelling of urban flooding. *Journal of Hydrology* **299** (3), 284–299.
- Martínez-Gomariz, E., Gómez, M. & Russo, B. 2016 Experimental study of the stability of pedestrians exposed to urban pluvial flooding. *Natural Hazards* **82** (2), 1259–1278.
- Merz, B., Kreibich, H., Schwarze, R. & Thieken, A. 2010 'Review article' assessment of economic flood damage. *Natural Hazards and Earth System Sciences* **10** (8), 1697.
- Mignot, E., Paquier, A. & Haider, S. 2006 Modeling floods in a dense urban area using 2D shallow water equations. *Journal of Hydrology* **327** (1), 186–199.
- Mignot, E., Paquier, A. & Rivière, N. 2008 Experimental and numerical modeling of symmetrical four-branch supercritical. *Journal of Hydraulic Research* **46** (6), 723–738.
- Moya Quiroga, V., Kure, S., Udo, K. & Mano, A. 2016 Application of 2D numerical simulation for the analysis of the February 2014 Bolivian Amazonia flood: application of the new HEC-RAS version 5. *RIBAGUA – Revista Iberoamericana del Agua* **3** (1), 25–33.
- Nie, L. 2016 Enhancing urban flood resilience – a case study for policy implementation. *Proceedings of the Institution of Civil Engineers – Water Management* **169** (2), 85–93.
- Nilsen, V., Lier, J. A., Bjerkholt, J. T. & Lindholm, O. G. 2011 Analysing urban floods and combined sewer overflows in a changing climate. *Journal of Water and Climate Change* **2** (4), 260–271.
- Noh, S. J., Lee, J.-H., Lee, S., Kawaike, K. & Seo, D.-J. 2018 Hyper-resolution 1D-2D urban flood modelling using LiDAR data and hybrid parallelization. *Environmental Modelling & Software* **103**, 131–145.
- Ozdemir, H., Sampson, C., de Almeida, G. A. & Bates, P. 2013 Evaluating scale and roughness effects in urban flood modelling using terrestrial LIDAR data. *Hydrology and Earth System Sciences* **10**, 5903–5942.
- Palmer, M. A., Reidy Liermann, C. A., Nilsson, C., Flörke, M., Alcamo, J., Lake, P. S. & Bond, N. 2008 Climate change and the world's river basins: anticipating management options. *Frontiers in Ecology and the Environment* **6** (2), 81–89.
- Patel, D. P., Ramirez, J. A., Srivastava, P. K., Bray, M. & Han, D. 2017 Assessment of flood inundation mapping of Surat city by coupled 1D/2D hydrodynamic modeling: a case application of the new HEC-RAS 5. *Natural Hazards* **89** (1), 93–130.
- Russo, B., Suñer, D., Velasco, M. & Djordjević, S. 2012 Flood hazard assessment in the Raval District of Barcelona using a 1D/2D coupled model. In *Proceedings of 9th International Conference on Urban Drainage Modelling*, Belgrade, Serbia. Faculty of Civil Engineering, University of Belgrade.
- Russo, B., Gómez, M. & Macchione, F. 2013 Pedestrian hazard criteria for flooded urban areas. *Natural Hazards* **69** (1), 251–265.
- Ryberg, K. R., Lin, W. & Vecchia, A. V. 2012 Impact of climate variability on runoff in the North-Central United States. *Journal of Hydrologic Engineering* **19** (1), 148–158.
- Singh, S. K. 2005 Clark's and Espey's unit hydrographs vs the gamma unit hydrograph/Les hydrogrammes unitaires de Clark et de Espey vs l'hydrogramme unitaire de forme loi gamma. *Hydrological Sciences Journal* **50** (6), 1067.

- The City of Copenhagen 2012 *Cloudburst Management Plan 2012, Technical and Environmental Administration*, pp. 6, 11 and 12. Available from [https://en.klimatilpasning.dk/media/665626/cph\\_-\\_cloudburst\\_management\\_plan.pdf](https://en.klimatilpasning.dk/media/665626/cph_-_cloudburst_management_plan.pdf).
- Turner, A., Colby, J., Csontos, R. & Batten, M. 2013 Flood modeling using a synthesis of multi-platform LiDAR data. *Water* **5** (4), 1533.
- Villarreal, E. L., Semadeni-Davies, A. & Bengtsson, L. 2004 Inner city stormwater control using a combination of best management practices. *Ecological Engineering* **22** (4), 279–298.
- Vojinovic, Z. & Tutulic, D. 2009 On the use of 1D and coupled 1D-2D modelling approaches for assessment of flood damage in urban areas. *Urban Water Journal* **6** (3), 183–199.

First received 16 May 2019; accepted in revised form 29 March 2020. Available online 4 May 2020